

Statistical Analysis on Random Quantum Sampling by Sycamore and Zuchongzhi Quantum Processors

Sangchul Oh* and Sabre Kais†

*Department of Chemistry, Department of Physics and Astronomy,
and Purdue Quantum Science and Engineering Institute, Purdue University, West Lafayette, IN, USA*

(Dated: April 13, 2022)

Random quantum sampling, a task to sample bit-strings from a random quantum circuit, is considered one of suitable benchmark tasks to demonstrate the outperformance of quantum computers even with noisy qubits. Recently, random quantum sampling was performed on the Sycamore quantum processor with 53 qubits [Nature **574**, 505 (2019)] and on the Zuchongzhi quantum processor with 56 qubits [Phys. Rev. Lett. **127**, 180501 (2021)]. Here, we analyze and compare statistical properties of the outputs of random quantum sampling by Sycamore and Zuchongzhi. Using the Marchenko-Pastur law and the Wasserstein distances, we find that quantum random sampling of Zuchongzhi is more closer to classical uniform random sampling than those of Sycamore. Some Zuchongzhi's bit-strings pass the random number tests while both Sycamore and Zuchongzhi show similar patterns in heatmaps of bit-strings. It is shown that statistical properties of both random quantum samples change little as the depth of random quantum circuits increases. Our findings raise a question about computational reliability of noisy quantum processors that could produce statistically different outputs for the same random quantum sampling task.

Introduction.— A quantum computer is believed to simulate quantum systems much better [1] and to solve some computational tasks exponentially faster [2, 3] than a classical computer. A demonstration of the outperformance of a quantum computer, called quantum supremacy [4] or quantum advantage, is considered one of the important milestones in developing practical quantum computers. Random quantum sampling [5] is regarded as a good candidate for demonstrating quantum advantage with noisy intermediate-scale quantum (NISQ) computers available these days. Recently, quantum advantage has been claimed for random quantum sampling on the Sycamore quantum processor with 53 superconducting qubits [6] and the Zuchongzhi quantum processor with 56 superconducting qubits [7], and for Boson sampling with optical qubits [5, 8, 9].

Quantum advantages of the Sycamore and Zuchongzhi quantum processors over classical computers for random quantum sampling were verified using the linear cross-entropy benchmarking (XEB) fidelity, whose values were estimated slightly larger than zero [6, 7]. Both quantum processors are made of two-dimensional arrays of superconducting transmon qubits, have similar error rates, executed the same random quantum circuit, and scored similar XEB values. So, one may speculate that the output bit-strings generated by the two noisy quantum processors would be statistically close. However, it is unknown whether two noisy quantum processors with similar values of the XEB fidelity sample statistically similar bit-strings or not. In this paper, we analyze the statistical closeness of the outputs of the two noisy quantum processors using the NIST random number tests [10], the Marchenko-Pastur distribution of eigenvalues of random matrices of bit-strings [11], and the Wasserstein distance between samples [12]. We show that Sycamore's random

bit-strings are farther away from classical uniform random bit-strings than Zuchongzhi's outputs, that is, the two outputs of bit-strings are noticeably different.

Random quantum sampling.— Let us first summarize random quantum sampling implemented on the Sycamore and Zuchongzhi quantum processors [6, 7]. The task of random quantum sampling is to sample bit-strings $x = a_1 \cdots a_n \in \{0, 1\}^n$ by applying a random quantum circuit U on the initial state $|0\rangle$ of n qubits followed by the measurement. Both Sycamore and Zuchongzhi quantum processors executed the same random quantum circuit U composed of m cycles as follows. A quantum circuit U_k at the k -th cycle consists of single-qubit gates R selected randomly from the set $\{\sqrt{X}, \sqrt{Y}, \sqrt{W}\}$ on all qubits and deterministic two-qubit gates on the pair of qubits selected in the sequence of the coupler activation patterns of 2-dimensional superconducting qubits. After m cycles, a final single-qubit gate R is applied before the measurement, so the whole random quantum circuit with cycle m is given by $U = RU_m U_{m-1} \cdots U_1$. The output of the random quantum circuit is a bit-string x that is sampled from the probability $p(x) = |\langle x | U | 0 \rangle|^2$. By implementing the same random quantum circuit M times, a collection of M random bit-strings $\mathcal{D} = \{x_1, \dots, x_M\}$, i.e., an $M \times n$ binary bit array, is obtained.

To verify that a noisy quantum processor is performing well random quantum sampling [6, 7], the linear cross-entropy benchmarking (XEB) fidelity F_{XEB} is introduced

$$F_{\text{XEB}} = 2^n \cdot \frac{1}{M} \sum_{x \in \mathcal{D}} p(x) - 1, \quad (1)$$

where the ideal probability $p(x) = |\langle x | U | 0 \rangle|^2$ of finding a bit-string x is computed on a classical computer using Schrödinger or Feynman simulators and the bit-strings

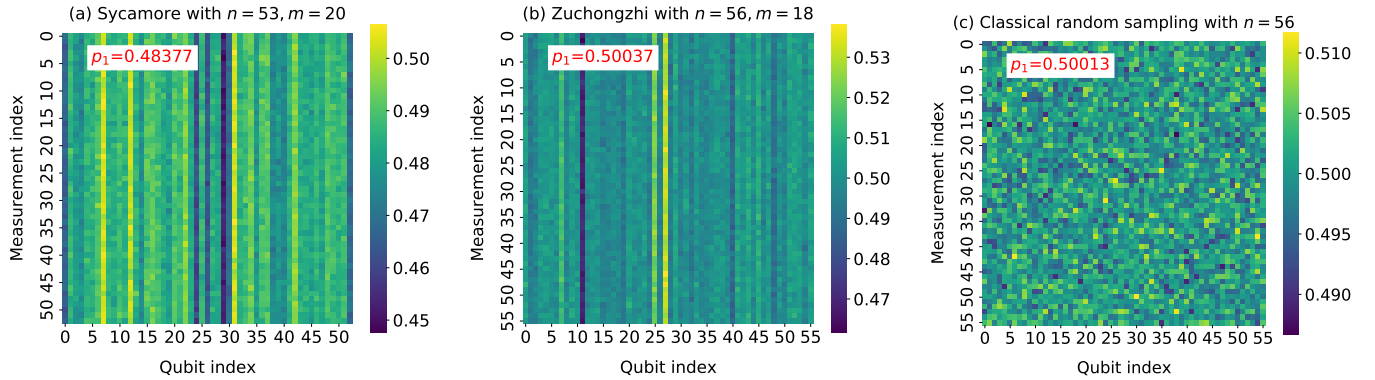


FIG. 1. Heatmaps of quantum random sampling (a) by the Sycamore quantum processor with $n = 53$ qubits, $m = 20$ cycles, and sample numbers $M = 10^6$, (b) by the Zuchongzhi quantum processor with $n = 56$ qubits, $m = 20$ cycles, and $M = 10^6$ samples, and (c) of classical uniform random sampling with $n = 56$ and $M = 10^6$ are plotted. The average of finding bit 1 is denoted by p_1 . Random quantum samples, (a) and (b), show the stripe patterns at specific qubit indices while (b) and (c) pass the NIST random number tests.

$\mathcal{D} = \{x_1, \dots, x_M\}$ are generated by a quantum processor. It is known that $F_{XEB} = 1$ if a quantum processor implements a random quantum circuit without errors, and $F_{XEB} = 0$ if bit-strings are sampled from a classical uniform distribution. The estimated XEB fidelity of Sycamore is $F_{XEB} = (2.24 \pm 0.021) \times 10^{-3}$ for 53 qubits, 20 cycles, and $M = 30 \times 10^6$ samples over 10 circuit instances [6]. For the Zuchongzhi quantum processor [7], the estimated XEB fidelity is $F_{XEB} = (6.62 \pm 0.72) \times 10^{-4}$ for 56 qubits, 20 cycles, and $M = 1.9 \times 10^7$ samples.

While the XEB fidelity could serve as a benchmark for quantum advantage of random quantum sampling, it has some limitations. The XEB fidelity stems from the Kullback-Leibler divergence or the cross entropy of an empirical probability distribution $\tilde{p}(x)$ of the data \mathcal{D} from the ideal probability distribution $p(x)$ [13]. As the number of qubits increases, it is very difficult to calculate both probability distributions. The number of samples required to construct the empirical probability $\tilde{p}(x)$ increases exponentially because the range of $x \in [0, 2^n - 1]$ does so. While the XEB fidelity needs only an ideal probability $p(x)$ but not $\tilde{p}(x)$, it is still not scalable because in quantum advantage regime a supercomputer cannot calculate the ideal probability $p(x)$ in Eq. (1) and no other NISQ processors could do. Recently, the limitation of the XEB fidelity as a benchmark for quantum advantage have been pointed out by Gao *et. al.* [14]. More importantly, the XEB fidelity could not give any clue about statistical properties of bit-strings of random quantum sampling implemented on NISQ processors.

Comparison of random quantum sampling of Sycamore and Zuchongzhi.— A simple way of comparing the performance of two quantum processors is to compare directly their outputs of a task, here random quantum sampling. Both Sycamore and Zuchongzhi have similar noise levels. The averages of single-qubit gate errors, two-qubit gates errors, and the readout error of Sycamore is about

0.15%, 0.36%, and 3.1%, respectively [6]. The average errors of Zuchongzhi are about 0.14% for single-qubit gates, 0.59% for two-qubit gates, and 4.52% for readout, respectively [7]. Both processors implemented the same random quantum circuit as described before and obtained similar values of XEB fidelity. So, one may expect that their outputs would be statistically close each other. However, that is not the case.

We first examine whether the output bit-strings of random quantum sampling are random. Random numbers have many practical applications in Monte-Carlo simulation, statistics, cryptography, etc.. Given a random quantum circuit U , the probability $p(x) = |\langle x | U | 0 \rangle|^2$ of finding bit-string x is not uniform due to the entanglement and interference, so some bit-strings are sampled more likely than others. However, there is no physical ground that the output of bit-strings $\mathcal{D} = \{x_1, x_2, \dots, x_M\}$ would contain more bit 1 than 0 or vice versa. Bits 0 and 1 are equally probable if there is no error. To see this, the output of bit-strings \mathcal{D} is sliced into the collection of $n \times n$ binary arrays, with which the heatmaps are plotted as shown in Fig. 1. Fig. 1 (a) depicts the heat map of Sycamore's bit-strings for $n = 53$ qubits, $m = 20$ cycles, and $M = 3 \times 10^6$ samples [15]. Fig. 1 (b) displays the heatmap of Zuchongzhi's bit-strings for $n = 56$ qubits, $m = 18$ cycles, and $M = 3 \times 10^6$ samples. Fig. 1 (c) shows the heatmap of uniform random bits sampled from a classical computer for $n = 56$ and $M = 3 \times 10^6$. As depicted in Fig. 1, the heatmaps of random quantum sampling on Sycamore and Zuchongzhi quantum processors show bright and dark stripes at some qubit indices while the classical uniform random sampling does not. One may suspect that stripe patterns could be caused by readout errors. However, for both Sycamore and Zuchongzhi data sets, the locations of bright or dark stripes in the heatmaps do not coincide with the indices of qubits with high readout errors.

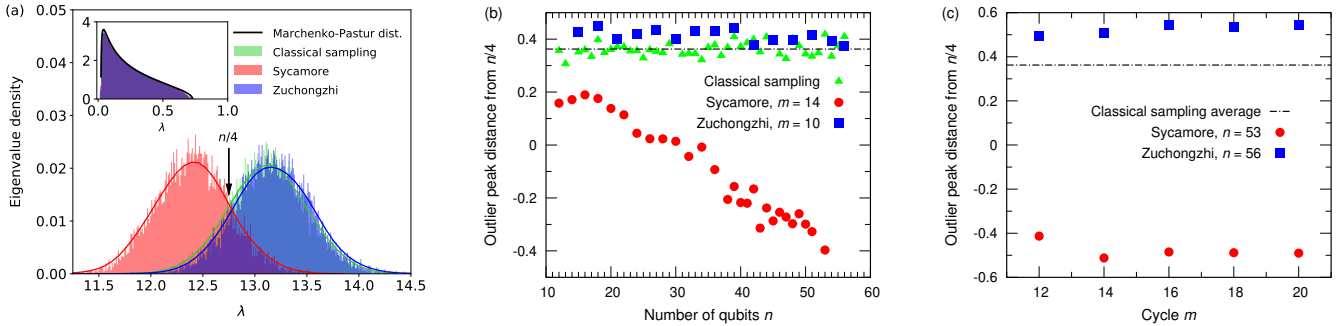


FIG. 2. (a) For $n = 51$ qubits, the outliers of the Marchenko-Pastur distributions of eigenvalues of classical random bit-strings (green), Sycamore’s quantum random bit-strings (red), and Zuchongzhi’s quantum random bit-strings (blue) are plotted. The inset of (a) depicts the bulk distribution of eigenvalues of the Marchenko-Pastur law given by Eq. (3). (b) The distances of the outlier peaks of Sycamore (red solid circle), Zuchongzhi (blue solid square), and classical random sampling (green triangle) from $n/4$ are plotted as a function of the qubit number n . (c) The distances of the peaks of Sycamore with $n = 53$ (solid red circle) and Zuchongzhi with $n = 56$ (blue solid square) from $n/4$ is plotted as a function of cycle m . The dot-dash lines in (b) and (c) represent the average distance of classical random sampling from $n/4$.

We count the number of bit 1 contained in the output bit-strings $\mathcal{D} = \{x_1, \dots, x_M\}$. The average of finding bit 1 is denoted by p_1 . Most Zuchongzhi outputs show p_1 is greater than 1/2, as shown in Supplementary Material [16], while all Sycamore outputs have p_1 less than 1/2 [17]. As depicted in Fig. 1, Zuchongzhi’s bit-strings with $n = 56$ qubits, $m = 18$ cycles has $p_1 = 0.50094$ while Sycamore’s bit-strings for $n = 53$ qubits and $m = 20$ cycles has $p_1 = 0.48383$. Note that the readout errors of Sycamore and Zuchongzhi are reported to be 3.1% and 4.52%, respectively. It is unclear why Sycamore and Zuchongzhi are quite different in the probability p_1 of finding bit 1 in random quantum sampling.

To see the randomness of bit-strings, we perform the NIST random number tests [10] for Zuchongzhi’s outputs. We find that some Zuchongzhi data sets pass the NIST random number tests while all Sycamore data sets do not [16, 17]. Note that the probability p_1 of finding bit 1 is related to the frequency test of the NIST random number tests. It is interesting to see that some Zuchongzhi data sets pass the NIST random number tests while all random quantum sampling data of Sycamore and Zuchongzhi show the stripe patterns unlike the classical uniform random samples, as shown in Fig. 1. This implies random quantum sampling may be used to generate quantum random numbers [18, 19].

Both Sycamore and Zuchongzhi showed similar exponential decays of the XEB fidelity F_{XEB} as a function of qubit number n or cycle m [6, 7]. One obtains $F_{\text{XEB}} = 0$ if bit-strings are sampled from the classical uniform random distribution $p_{\text{cl}}(x) = 1/2^n$. Using the Marchenko-Pastur distribution [11] and the Wasserstein distances [12, 20], we examine how the random bit-string outputs of Sycamore and Zuchongzhi are far away from classical uniform random samples as a function of qubit number n and cycle m .

The signal out of randomness can be captured by the outliers of the Marchenko-Pastur distribution of random matrices. This method has been applied to the covariance matrices in finance [21, 22] in predicting ligand and affinity [23], and in denoising MRI [24] and single-cell data [25]. We use the Marchenko-Pastur distribution of eigenvalues of random bit-strings to measure the distance among Sycamore’s outputs, Zuchongzhi’s output, and classical uniform random samples. The data $\mathcal{D} = \{x_1, x_2, \dots, x_M\}$, an binary $M \times n$ array, is sliced into the collection of $k \times n$ random matrices X . All entries of X are assumed to be independent and identically binary random variable $\{0, 1\}$ with the mean $\mu_X = 1/2$ and the variance $\sigma_X^2 = 1/4$. We calculate the empirical distribution of eigenvalues of $n \times n$ matrix $\frac{1}{k}X^t \cdot X$, as shown in Fig. 2. The empirical eigenvalue distribution is composed of the two parts: the bulk corresponding to the noise or random and the outliers representing the signal. To understand this, let consider the transformed random matrix $Y = 2X - J$ with J of all entries 1. The matrix $\frac{1}{k}X^t \cdot X$ is written as

$$\frac{1}{k}X^t \cdot X = \frac{1}{4k} (Y^t \cdot Y + X^t \cdot J + X^t \cdot Z + J^t \cdot J). \quad (2)$$

The matrix Y has the mean $\mu_Y = 0$ and the variance $\sigma_Y^2 = 1$. The eigenvalue distribution of the first term in Eq. (2), $\frac{1}{k}Y^t \cdot Y$, follows the Marchenko-Pastur distribution [11]

$$\rho(\lambda) = \frac{1}{2\pi\sigma^2\gamma} \frac{\sqrt{(\lambda_+ - \lambda)(\lambda - \lambda_-)}}{\lambda}, \quad (3)$$

where $\gamma = n/k$ is the rectangular ratio and $\lambda_{\pm} = \sigma^2(1 \pm \sqrt{\gamma})^2$ are the upper and lower bounds. Here we take $k = 2n$, i.e., $\gamma = 1/2$. The upper limit is given by $\lambda_+ = 1 + \sqrt{1/2}$. By considering the scaling factor 1/4, the upper limit of $(1/4k) \cdot Y^t \cdot Y$ is given by $(1 + \sqrt{1/2})/4 \approx$

0.7285. The last term of Eq. (2), $(1/4k)J^t \cdot J$ has the two eigenvalues, 0 and $n/4$. So the outliers are located around $n/4$.

Fig. 2 (a) plots the empirical distribution of eigenvalues of $\frac{1}{k}X^t \cdot X$ made of Sycamore bit-strings with $n = 51$, $m = 14$, and $M = 10^6$ (red color), Zuchongzhi bit-strings with $n = 51$, $m = 10$ and $M = 10^6$ (blue color), and classical uniform random bits with $M = 10^6$ (green color). The outlier peak of Sycamore is located at the left of $n/4$ while the outlier peaks of Zuchongzhi and classical random sampling are located at right of $n/4$. Surprisingly, Zuchongzhi's bit-strings are more closer to the classical random bit strings than Sycamore's ones while Sycamore and Zuchongzhi have similar the values of the XEB fidelity. Fig. 2 (b) plots the distances of the outlier peaks from $n/4$ as a function of qubit number n . Sycamore becomes farther away from $n/4$ as n increases. On the other hands, Zuchongzhi's distance from $n/4$ changes a little. The XEB fidelity of Sycamore and Zuchongzhi decays exponentially as a function of qubit number n . Fig. 2 (c) plots the peak distance from $n/4$ as a function of cycles for Sycamore $n = 53$ and for Zuchongzhi $n = 56$. This result is also in contrast with the decay behavior of the XEB fidelity as a function of cycle m .

The statistical distances among Sycamore, Zuchongzhi, and classical random sampling, based on the Marchenko-Pastur distribution, can be further confirmed by calculating the Wasserstein distances. The 1-th Wasserstein distance between two probability distribution $p(x)$ and $q(x)$ [12] is defined by

$$W_p(p, q) = \inf_{\pi \in \Pi(p, q)} \mathbb{E}_{(x, y) \sim \pi} [| | | x - y | | |], \quad (4)$$

where $\Pi(p, q)$ is the set of all joint distribution $\pi(x, y)$ whose marginal distributions are $p(x)$ and $p(y)$, respectively. Given two samples, $\{x_1, x_2, \dots, x_M\}$ and $\{y_1, y_2, \dots, y_M\}$, $W(p, q)$ can be calculated directly without calculating the empirical distributions $p(x)$ and $q(x)$ [20]. The Wasserstein distance is a true metric on a probability space, so the relative Wasserstein distances among Sycamore, Zuchongzhi, and classical random sampling, give rise to the triangle inequality. Fig. 3 (a) plot the triangle relation among the three data sets for $n = 18, 24, 30, 36, 42, 45, 48, 51$. All Zuchongzhi data sets are close to classical random sampling than Sycamore. This is consistent with the outlier peak distances from $n/4$ of the Marchenko-Pastur distribution shown in Fig. 2 (b). Fig. 3 (b) plots the Wasserstein distance of Sycamore $n = 53$ and Zuchongzhi $n = 56$ from the classical random bit-strings as a function of cycle m . This result is consistent with the behavior of the relative distances of the outliers of the Marchenko-Paster distribution as a function of m , shown in Fig. 2 (c). Note that the Wasserstein distances between the bit-strings with different cycles of Sycamore (or Zuchongzhi) are less than the Wasserstein distance of them from the classical random sampling.

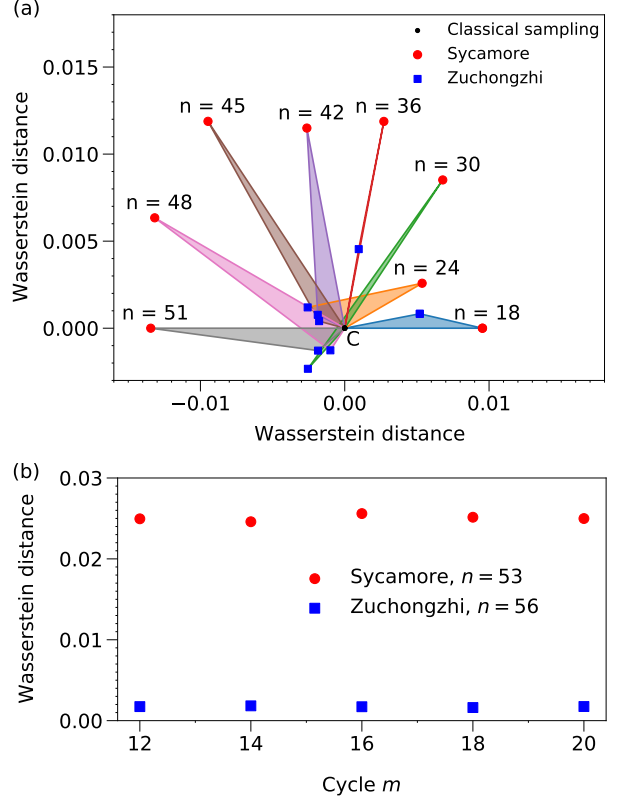


FIG. 3. (a) For qubits $n = 18, 24, 30, 36, 42, 45, 48, 51$, the relative positions of Sycamore (red circle), Zuchongzhi (blue square), and classical random sampling (black circle at origin) form triangles whose edges are the Wasserstein distances. For clarity, triangles are rotated. (b) for Sycamore bit-strings with $n = 53$ and Zuchongzhi with $n = 56$, the Wasserstein distances from the classical random sampling are plotted as a function of cycle m .

Conclusion.— In this paper, we analyzed the statistical properties of random bit-strings sampled from Sycamore and Zuchongzhi quantum processors using the heatmaps, the NIST random number tests, the Marchenko-Pastur distribution, and the Wasserstein distances. Both Sycamore and Zuchongzhi exhibit stripe patterns in the heatmaps of random bit-strings. Some of Zuchongzhi's data pass the NIST random number tests. This may open up a possibility of the use of the random quantum circuit as a quantum random number generator. The Marchenko-Pastur distribution and the Wasserstein distances of random bit-strings shows that Zuchongzhi random quantum sampling is statistically more closer to classical random sampling than Sycamore's, while both have similar error rates and similar values of the XEB fidelity. The distances of random bit-strings of Sycamore from the classical uniform sampling as a function of the number of qubit n is quite different from those of Zuchongzhi. The distances of Sycamore's and Zuchongzhi's bit-strings from the classical random bit-strings remain

almost constant as the cycle number m increases. This is in contrast with the exponential decay of the XEB fidelity as a function of m .

The results found here raise a question about computational reliability and verification of noisy quantum processors [26]. Two classical computers performing the same task will produce the same outputs (within statistical errors for stochastic calculation). One may expect that two NISQ processors with similar error rates would produce statistically close outputs. However, the results here show an exceptional case. In order to ensure the reliability of quantum computing with NISQ quantum processors, it is necessary to have good benchmark tools which can verify the output of quantum calculation on a classical computer, until fully-error corrected quantum computers are available.

We would like to thank the Google quantum team for making their random quantum sampling by Sycamore available. We also would like to thank Y. Wu and J.-W. Pan for providing us the data on Zuchongzhi [7]. This material is based upon work supported by the U.S. Department of Energy, Office of Science, National Quantum Information Science Research Centers. We also acknowledge the National Science Foundation under award number 1955907.

-
- * oh.sangchul@gmail.com
 † Corresponding author: kais@purdue.edu
- [1] R. P. Feynman, *International Journal of Theoretical Physics* **21**, 467 (1982).
 - [2] P. W. Shor, *SIAM Journal on Computing* **26**, 1484 (1997).
 - [3] A. W. Harrow, A. Hassidim, and S. Lloyd, *Phys. Rev. Lett.* **103**, 150502 (2009).
 - [4] J. Preskill, Quantum computing and the entanglement frontier (2012), arXiv:1203.5813 [quant-ph].
 - [5] S. Aaronson and A. Arkhipov, *Theory of Computing* **9**, 143 (2013).
 - [6] F. Arute, K. Arya, R. Babbush, D. Bacon, J. C. Bardin, R. Barends, R. Biswas, S. Boixo, F. G. S. L. Brandao, D. A. Buell, B. Burkett, Y. Chen, Z. Chen, B. Chiaro, R. Collins, W. Courtney, A. Dunsworth, E. Farhi, B. Foxen, A. Fowler, C. Gidney, M. Giustina, R. Graff, K. Guerin, S. Habegger, M. P. Harrigan, M. J. Hartmann, A. Ho, M. Hoffmann, T. Huang, T. S. Humble, S. V. Isakov, E. Jeffrey, Z. Jiang, D. Kafri, K. Kechedzhi, J. Kelly, P. V. Klimov, S. Knysh, A. Korotkov, F. Kostritsa, D. Landhuis, M. Lindmark, E. Lucero, D. Lyakh, S. Mandrà, J. R. McClean, M. McEwen, A. Megrant, X. Mi, K. Michelsen, M. Mohseni, J. Mutus, O. Naaman, M. Neeley, C. Neill, M. Y. Niu, E. Ostby, A. Petukhov, J. C. Platt, C. Quintana, E. G. Rieffel, P. Roushan, N. C. Rubin, D. Sank, K. J. Satzinger, V. Smelyanskiy, K. J. Sung, M. D. Trevithick, A. Vainsencher, B. Villalonga, T. White, Z. J. Yao, P. Yeh, A. Zalcman, H. Neven, and J. M. Martinis, *Nature* **574**, 505 (2019).
 - [7] Y. Wu, W.-S. Bao, S. Cao, F. Chen, M.-C. Chen, X. Chen, T.-H. Chung, H. Deng, Y. Du, D. Fan, M. Gong, C. Guo, C. Guo, S. Guo, L. Han, L. Hong, H.-L. Huang, Y.-H. Huo, L. Li, N. Li, S. Li, Y. Li, F. Liang, C. Lin, J. Lin, H. Qian, D. Qiao, H. Rong, H. Su, L. Sun, L. Wang, S. Wang, D. Wu, Y. Xu, K. Yan, W. Yang, Y. Yang, Y. Ye, J. Yin, C. Ying, J. Yu, C. Zha, C. Zhang, H. Zhang, K. Zhang, Y. Zhang, H. Zhao, Y. Zhao, L. Zhou, Q. Zhu, C.-Y. Lu, C.-Z. Peng, X. Zhu, and J.-W. Pan, *Phys. Rev. Lett.* **127**, 180501 (2021).
 - [8] H.-S. Zhong, H. Wang, Y.-H. Deng, M.-C. Chen, L.-C. Peng, Y.-H. Luo, J. Qin, D. Wu, X. Ding, Y. Hu, P. Hu, X.-Y. Yang, W.-J. Zhang, H. Li, Y. Li, X. Jiang, L. Gan, G. Yang, L. You, Z. Wang, L. Li, N.-L. Liu, C.-Y. Lu, and J.-W. Pan, *Science* **370**, 1460 (2020).
 - [9] H.-S. Zhong, Y.-H. Deng, J. Qin, H. Wang, M.-C. Chen, L.-C. Peng, Y.-H. Luo, D. Wu, S.-Q. Gong, H. Su, Y. Hu, P. Hu, X.-Y. Yang, W.-J. Zhang, H. Li, Y. Li, X. Jiang, L. Gan, G. Yang, L. You, Z. Wang, L. Li, N.-L. Liu, J. J. Renema, C.-Y. Lu, and J.-W. Pan, *Phys. Rev. Lett.* **127**, 180502 (2021).
 - [10] L. Bassham, A. Rukhin, J. Soto, J. Nechvatal, M. Smid, S. Leigh, M. Levenson, M. Vangel, N. Heckert, and D. Banks, *A statistical test suite for random and pseudorandom number generators for cryptographic applications* (2010).
 - [11] V. A. Marchenko and L. A. Pastur, *Mat. Sb. (N.S.)* **72**, 507 (1967).
 - [12] C. Villani, *Optimal Transport: Old and New*, Grundlehren der mathematischen Wissenschaften (Springer Berlin Heidelberg, 2008).
 - [13] S. Boixo, S. V. Isakov, V. N. Smelyanskiy, R. Babbush, N. Ding, Z. Jiang, M. J. Bremner, J. M. Martinis, and H. Neven, *Nature Physics* **14**, 595 (2018).
 - [14] X. Gao, M. Kalinowski, C.-N. Chou, M. D. Lukin, B. Barak, and S. Choi, Limitations of linear cross-entropy as a measure for quantum advantage (2021), arXiv:2112.01657 [quant-ph].
 - [15] J. M. Martinis *et al.*, Quantum supremacy using a programmable superconducting processor, dryad, dataset (2021).
 - [16] See Supplemental Material for the details of calculation.
 - [17] S. Oh and S. Kais, Non-randomness of google’s quantum supremacy benchmark (2021), arXiv:2110.06046 [quant-ph].
 - [18] M. Herrero-Collantes and J. C. Garcia-Escartin, *Rev. Mod. Phys.* **89**, 015004 (2017).
 - [19] K. Tamura and Y. Shikano, in *International Symposium on Mathematics, Quantum Theory, and Cryptography*, edited by T. Takagi, M. Wakayama, K. Tanaka, N. Kunihiro, K. Kimoto, and Y. Ikematsu (Springer Singapore, Singapore, 2021) pp. 17–37.
 - [20] R. Flamary, N. Courty, A. Gramfort, M. Z. Alaya, A. Boisbunon, S. Chambon, L. Chapel, A. Corenflos, K. Fatras, N. Fournier, L. Gautheron, N. T. Gayraud, H. Janati, A. Rakotomamonjy, I. Redko, A. Rolet, A. Schutz, V. Seguy, D. J. Sutherland, R. Tavenard, A. Tong, and T. Vayer, *Journal of Machine Learning Research* **22**, 1 (2021).
 - [21] L. Laloux, P. Cizeau, J.-P. Bouchaud, and M. Potters, *Phys. Rev. Lett.* **83**, 1467 (1999).
 - [22] L. Laloux, P. Cizeau, M. Potters, and J.-P. Bouchaud, *International Journal of Theoretical and Applied Finance* **03**, 391 (2000).

- [23] A. A. Lee, M. P. Brenner, and L. J. Colwell, *Proceedings of the National Academy of Sciences* **113**, 13564 (2016).
- [24] J. Veraart, E. Fieremans, and D. S. Novikov, *Magnetic Resonance in Medicine* **76**, 1582 (2016), <https://onlinelibrary.wiley.com/doi/pdf/10.1002/mrm.26059>.
- [25] L. Aparicio, M. Bordyuh, A. J. Blumberg, and R. Rabadan, *Patterns* **1**, 100035 (2020).
- [26] J. Eisert, D. Hangleiter, N. Walk, I. Roth, D. Markham, R. Parekh, U. Chabaud, and E. Kashefi, *Nature Reviews Physics* **2**, 382 (2020).

**SUPPLEMENTARY MATERIAL:
STATISTICAL ANALYSIS ON RANDOM QUANTUM SAMPLING BY SYCAMORE AND
ZUCHONGZHI QUANTUM PROCESSORS**

Sangchul Oh and Sabre Kais

Supplemental material presents the heatmaps and the NIST random number tests for random bit-strings of Zuchongzhi. The Wasserstein distances among different cycles for Sycamore and Zuchongzhi are presented.

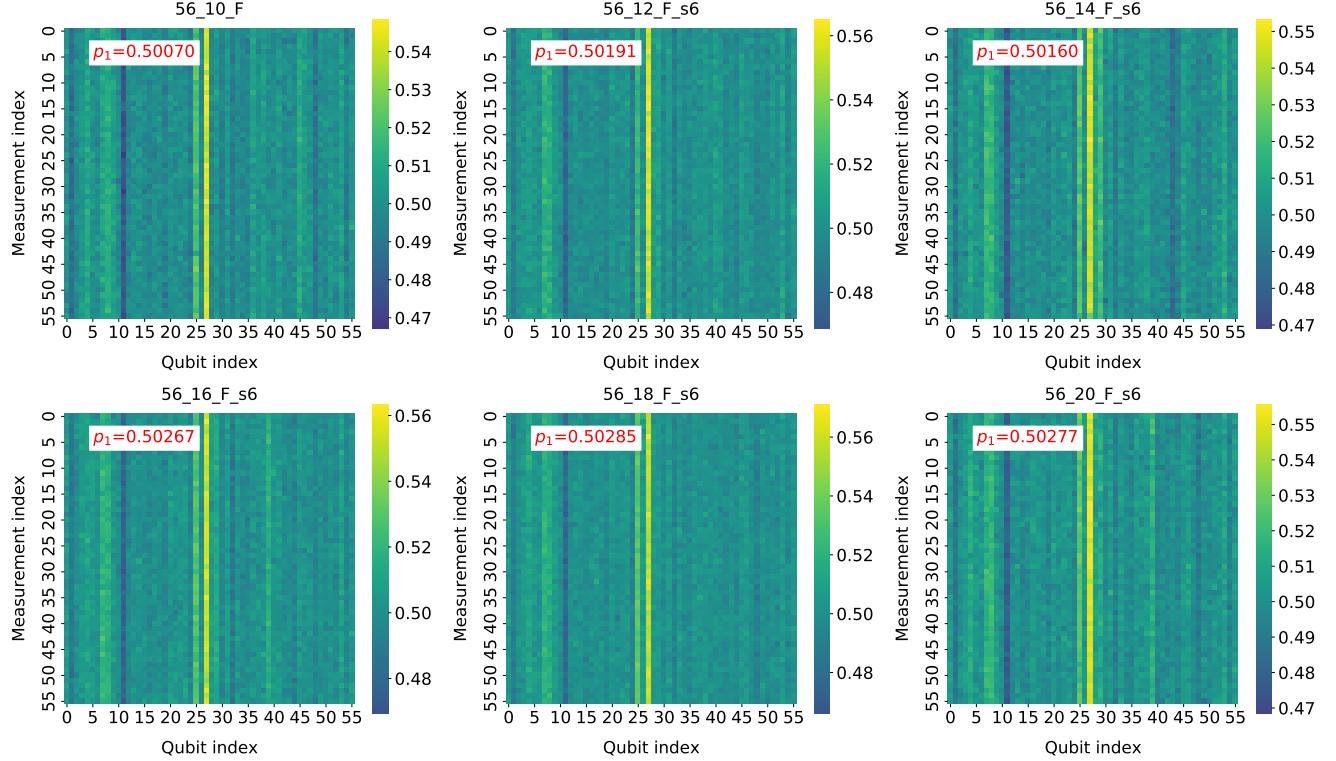


FIG. 4. Heatmaps of random bit-strings of Zuchongzhi with $n = 56$ and $m = 10, 12, 14, 16, 18, 20$.

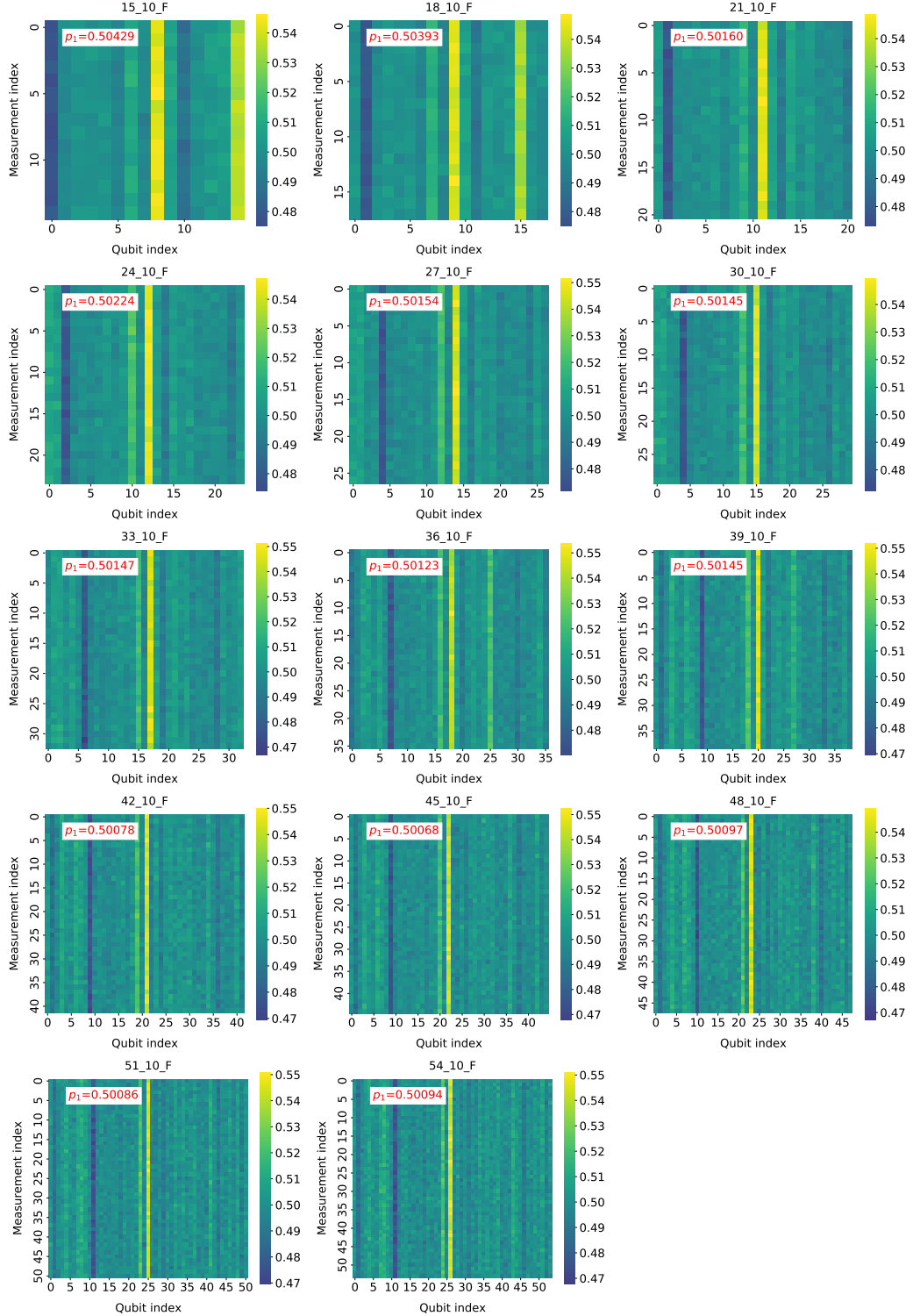


FIG. 5. Heatmaps of random bit-strings of Zuchongzhi with $n = 15, 18, 21, \dots, 51$ and $m = 10$.

File name	M	p_1	NIST random number tests
15_10_F.csv	1000000	0.5042914666666667	Nonrandom
18_10_F.csv	1000000	0.5039382222222222	Nonrandom
21_10_F.csv	1000000	0.5016010476190477	Nonrandom
24_10_F.csv	1000000	0.502242875	Random
27_10_F.csv	1000000	0.5015492592592593	Random
30_10_F.csv	1000000	0.5014525333333333	Random
33_10_F.csv	1000000	0.5014795757575757	Nonrandom
36_10_F.csv	1000000	0.5012370277777778	Nonrandom
39_10_F.csv	1000000	0.5014506153846154	Random
42_10_F.csv	1000000	0.5007865238095238	Nonrandom
45_10_F.csv	1000000	0.5006884222222222	Random
48_10_F.csv	1000000	0.5009762291666666	Random
51_10_F.csv	1000000	0.5008632549019608	Nonrandom
54_10_F.csv	1050000	0.5009445502645503	Nonrandom
56_10_F.csv	1170000	0.5007047619047619	Random

TABLE I. NIST random number tests for random bit-strings of Zuchongzhi with $n = 15, \dots, 56$ and $m = 10$. M stands for the number of bit-strings and p_1 for the probability of finding bit 1. 5 data files in directories, a_1, a_2, a_3, a_4, a_5 , are merged into a single file. Nonrandom means that bit-strings fail some of the NIST random tests.

Test Data File:/home/soh/Desktop/data/Zuchongzhi_nxx_m10/56_10_F_1M.csv

Type of Test	P-Value	Conclusion
01. Frequency Test (Monobit)	0.04725583993159622	Random
02. Frequency Test within a Block	0.7377345740502045	Random
03. Run Test	0.9013653598338198	Random
04. Longest Run of Ones in a Block	0.5576699582990581	Random
05. Binary Matrix Rank Test	0.13573737861315063	Random
06. Discrete Fourier Transform (Spectral) Test	0.4912971242158931	Random
07. Non-Overlapping Template Matching Test	0.7861450901488796	Random
08. Overlapping Template Matching Test	0.3562201622350592	Random
09. Maurer's Universal Statistical test	0.18901932905865293	Random
10. Linear Complexity Test	0.6012867491687948	Random
11. Serial test:		
	0.9287873362845678	Random
	0.6473140941950127	Random
12. Approximate Entropy Test	0.9658862333540649	Random
13. Cummulative Sums (Forward) Test	0.08552956685396966	Random
14. Cummulative Sums (Reverse) Test	0.09230410462727737	Random
15. Random Excursions Test:		
State	Chi Squared	P-Value
-4	2.2829376648618633	0.8087695808555937
-3	2.9604	0.706091109222725
-2	5.783950617283951	0.3278123367522591
-1	6.75	0.23990688227010742
+1	2.9166666666666667	0.7128316836671243
+2	1.876543209876543	0.8659503247833513
+3	2.6755999999999998	0.7498477047163237
+4	4.022629459947245	0.5461624839081891
16. Random Excursions Variant Test:		
State	COUNTS	P-Value
-9.0	6	0.5286121252556878
-8.0	9	0.5761501220305789
-7.0	17	0.7793054481711047
-6.0	21	0.8961247779728454
-5.0	12	0.5637028616507731
-4.0	11	0.47819532084058625
-3.0	14	0.5186050164287256
-2.0	17	0.5596689271994115
-1.0	19	0.47048642205878966
+1.0	29	0.47048642205878966
+2.0	33	0.4532547047537364
+3.0	49	0.1065831695748876
+4.0	56	0.08085559837005228
+5.0	60	0.08326451666355045
+6.0	64	0.08172275229865938
+7.0	63	0.11846489387154538
+8.0	58	0.20511768103340522
+9.0	39	0.5995101785600032

TABLE II. Result of the NIST random number tests for Zuchongzhi's data 56-10-F.csv.

File name	M	p_1	NIST random number tests
56_12_F_s11.csv	1000000	0.5004180892857143	Nonrandom
56_12_F_s12.csv	1000000	0.4997393035714286	Random
56_12_F_s13.csv	1000000	0.5016109285714285	Nonrandom
56_12_F_s15.csv	1000000	0.5005064107142857	Random
56_12_F_s3.csv	1000000	0.5004619464285714	Random
56_12_F_s4.csv	1000000	0.5015308571428572	Nonrandom
56_12_F_s5.csv	1000000	0.5012426964285714	Random
56_12_F_s6.csv	1000000	0.5019179107142857	Random
56_12_F_s8.csv	980000	0.5011627733236151	Random
56_12_F_s9.csv	1000000	0.5012499464285715	Nonrandom
56_14_F_s11.csv	1370000	0.502104027632951	Nonrandom
56_14_F_s12.csv	1440000	0.5003947048611112	Nonrandom
56_14_F_s13.csv	1700000	0.5007865021008403	Nonrandom
56_14_F_s15.csv	1120000	0.5003659757653062	Nonrandom
56_14_F_s3.csv	1100000	0.5011199512987013	Nonrandom
56_14_F_s4.csv	1290000	0.5018366832779624	Nonrandom
56_14_F_s5.csv	1310000	0.5014550572519084	Nonrandom
56_14_F_s6.csv	1400000	0.5016173852040816	Nonrandom
56_14_F_s8.csv	1480000	0.5015874396718146	Nonrandom
56_14_F_s9.csv	1390000	0.5016998843782117	Nonrandom
56_16_F_s11.csv	3560000	0.501555216693419	Nonrandom
56_16_F_s12.csv	3770000	0.5006029840848807	Random
56_16_F_s13.csv	3680000	0.5012373495729814	Nonrandom
56_16_F_s15.csv	2870000	0.5008621329019413	Nonrandom
56_16_F_s3.csv	2890000	0.5017474913494809	Nonrandom
56_16_F_s4.csv	3200000	0.5013628404017857	Nonrandom
56_16_F_s5.csv	2920000	0.5025822773972602	Nonrandom
56_16_F_s6.csv	3570000	0.5023631752701081	Nonrandom
56_16_F_s8.csv	3710000	0.5017546592221794	Nonrandom
56_16_F_s9.csv	3420000	0.5018155127401838	Nonrandom
56_18_F_s11.csv	10080000	0.5012828125	Nonrandom
56_18_F_s12.csv	9730000	0.5006819630010277	Random
56_18_F_s13.csv	11530000	0.5014127137281625	Nonrandom
56_18_F_s15.csv	9530000	0.5014926154249738	Random
56_18_F_s3.csv	7660000	0.5021444307161507	Nonrandom
56_18_F_s4.csv	7510000	0.5024223606619745	Nonrandom
56_18_F_s5.csv	7960000	0.5020297963029433	Nonrandom
56_18_F_s6.csv	9390000	0.5027202723261829	Nonrandom
56_18_F_s8.csv	8620000	0.501850381173351	Nonrandom
56_18_F_s9.csv	7470000	0.5023868091413272	Nonrandom
56_20_F_s11.csv	27900000	0.5018168573988735	Nonrandom
56_20_F_s12.csv	25870000	0.5013624744602132	Nonrandom
56_20_F_s13.csv	26580000	0.5017120135977642	Nonrandom
56_20_F_s15.csv	20100000	0.5013940840440654	Nonrandom
56_20_F_s3.csv	19100000	0.502459691473448	Nonrandom
56_20_F_s4.csv	21510000	0.5024990527661553	Nonrandom
56_20_F_s5.csv	22570000	0.502620922102664	Nonrandom
56_20_F_s6.csv	24510000	0.5030497945445008	Nonrandom
56_20_F_s8.csv	19840000	0.5022362093173963	Nonrandom
56_20_F_s9.csv	23510000	0.5026191111684998	Nonrandom

TABLE III. NIST random number tests for random bit-strings of Zuchongzhi with $n = 56$ and $m = 12, 14, 16, 18, 20$. M stands for the number of bit-strings and p_1 for the probability of finding bit 1. Nonrandom means that bit-strings fail some of the NIST random tests.

	classical n53	n53-m12	n53-m14	n53-m16	n53-m18	n53-m20
classical n53	0.0	0.02495338	0.02459099	0.02560033	0.02514710	0.0249869
n53-m12	0.02495337	0.0	0.00083951	0.00040303	0.00050475	0.0005789
n53-m14	0.02459099	0.00083951	0.0	0.00099459	0.00128885	0.0013602
n53-m16	0.02560033	0.00040303	0.00099459	0.0	0.00066794	0.0007389
n53-m18	0.02514710	0.00050475	0.00128885	0.00066794	0.0	0.0002826
n53-m20	0.02498690	0.00057892	0.00136027	0.00073890	0.00028265	0.0

TABLE IV. For $n = 53$, the Wasserstein distances among classical random bit-strings and Sycamore random bit-strings with cycle $m = 12, 14, 16, 18, 20$. The Wasserstein distance between the classical random bit-strings and Sycamore's random bit-strings is much larger than those between Sycamore's random bit-strings with different cycle.

	classical n56	n56-m12	n56-m14	n56-m16	n56-m18	n56-m20
classical n56	0.0	0.00173514	0.00183101	0.00171989	0.00161961	0.00174550
n56-m12	0.00173514	0.0	0.00071221	0.00023922	0.00056779	0.00034071
n56-m14	0.00183101	0.00071221	0.0	0.00085164	0.00125725	0.00073764
n56-m16	0.00171989	0.00023922	0.00085164	0.0	0.00045474	0.00025549
n56-m18	0.00161961	0.00056779	0.00125725	0.00045474	0.0	0.00056125
n56-m20	0.00174550	0.00034071	0.00073764	0.00025549	0.00056125	0.0

TABLE V. For $n = 56$, the Wasserstein distances among classical random bit-strings and Zuchongzhi random bit-strings with cycle $m = 12, 14, 16, 18, 20$.